



# Numerical Investigation of the Influence of Axial Overlap of Blade Angle Slots on an Axial Flow Compressor Stability

H. Zhang<sup>1</sup>, W. Liu<sup>1†</sup>, E. Wang<sup>1</sup>, W. Chu<sup>1</sup>, J. Yang<sup>2</sup> and W. Zhao<sup>2</sup>

<sup>1</sup> School of Power and Energy, Northwestern Polytechnical University, Xi'an, Shaanxi, 710129, China

<sup>2</sup> AECC Hunan Aviation Powerplant Research Institute, Zhuzhou, Hunan, 412002, China

†Corresponding Author Email: [whliu@mail.nwpu.edu.cn](mailto:whliu@mail.nwpu.edu.cn)

(Received November 16, 2019; accepted May 5, 2020)

## ABSTRACT

In this paper, a numerical investigation was conducted on a subsonic compressor rotor with blade angle slot casing treatments. The purpose of the investigation is to reveal the influence of axial overlap of blade angle slot on the compressor stability. Six kinds of blade angle slot casing treatments with different axial overlap rates were investigated in this paper. The results show that with the increasing of axial overlap rates, the stall margin improvement firstly increased and then decreased. And the optimal blade angle slot can obtain 62.51% improvement of stall margin. The flow field analyses show that the bleeding flows formed inside slots can restrain the adverse tip leakage flow, which is the critical factor making the onset of the rotor stall. With the increasing of axial overlap rate of the slots, the relative position between bleeding flows in the slots and tip leakage flow plays an important role in the stall margin improvement.

**Keywords:** Compressor; Casing treatment; Slots; Stability; Axial overlap.

## NOMENCLATURE

AS	Blade angle Slots	M	mass flow rate
CT	Casing Treatment	$V_r$	radial velocity
DMF	Dimensionless Mass Flow rate	$V_z$	axial velocity
TLF	Tip clearance Leakage Flow	$\pi^*$	absolute total pressure ratio
PEL	Peak Efficiency Loss	$\eta^*$	rotor efficiency
SW	Smooth Wall		
SMI	Stall Margin Improvement		

## 1. INTRODUCTION

In the aero-engine, the stall and surge are two critical problems, which are harmful to the compressor stability (Benser and Finger 1957; Greitzer 1976a, b). In order to solve the threat of stall and surge to compressor stability, casing treatments, as a kind of passive control methods, was discovered to delay the inception of stall and surge (Koch 1970). The types of casing treatment mainly contain the circumferential grooves and slots. In general, the slots can obtain larger stall margin improvement with greater sacrifice of the efficiency than circumferential grooves (Prince *et al.* 1975; Lin *et al.* 2008; Muller *et al.* 2011). Due to

the excellent capacity of extending stall margin, the slots are widely investigated. The mechanism of extending stall margin about slots has been revealed by numerical and experimental methods (Hembera *et al.* 2008; Brignole *et al.* 2008; Brandstetter *et al.* 2016). The slots can reduce and restrain the tip leakage vortex, which is a critical incentive in the process of the stall inception. To guide the design of slots, many investigations about slot configurations and parameters are carried out.

Fujita and Takata (1984) tested a series of configurations of slots in an experiment, like axial overlap, axial position, axial and radial skew. The experimental results were used to guide the optimization design of slots. Guruprasad (1999)

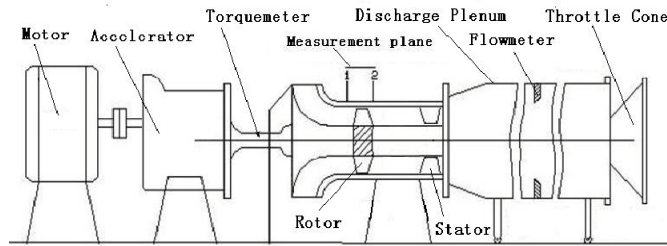


**Fig. 1. Structure diagram of the test rig.**

carried out an experimental study for different axial coverages of slots. An optimum axial coverage had been revealed. [Wike and Kau \(2003\)](#) conducted a numerical investigation about the effect of axial slots on the compressor stability and efficiency. Two different axial positions of slots were investigated. For the first position, the slots cover the blade tip from the leading edge to the trailing edge; for the second position, the slots were shifted upstream and covers about 25% the blade tip chord. The results show that the two kinds of slots can significantly increase the stall margin, whereas the slots shifted upstream generates an improvement of efficiency. Another numerical investigation carried out by [Wike \*et al.\* \(2005\)](#) also indicates that the slots positioned more upstream cause less decrease on the efficiency. [Danner \*et al.\* \(2009\)](#) performed an experimental and numerical study on the axial position of axial slots, three different slots with small, medium and large overlap were designed. The results reveal that the slots with small overlap can obtain the largest stall margin improvement and the least penalty in the efficiency. [Djeghri \*et al.\* \(2015\)](#) performed a parametric study for slots casing treatment in a mixed-flow compressor rotor. Many structural parameters of slots were investigated, like axial position, axial length, skew angle and so on. They concluded that the axial position has a minor effect on the stall margin, and the slots positioned more downstream cause more decrease on the efficiency. [Liu \*et al.\* \(1987\)](#) and [Zhang \*et al.\* \(2011\)](#) found that the slots shifted upstream can decrease the drop of the efficiency with acceptable stall margin improvement. However, the slots shifted downstream reduce the stall margin improvement and also decrease the drop of the efficiency. [Zhu \*et al.\* \(2005\)](#) and [Lu \*et al.\* \(2006\)](#) studied the bend skew slot in a subsonic compressor, and found that the axial position of slots is the most important factor of affecting the efficiency. In the process of designing slots, the axial position should cover the initial location of the tip leakage vortex, and it was revealed by [Lu \*et al.\* \(2009\)](#). The investigations carried out by [Kuang \*et al.\* \(2017\)](#) and [Zhou \*et al.\* \(2017\)](#) indicate that the axial position of slots has a great effect on the compressor stability and efficiency. And [Zhou \*et al.\* \(2017\)](#) concluded that the slots should cover the initial location of the tip leakage vortex and the boundary layer separation zone.

After reviewing the past studies on slots, we can know that the axial position has great effects on the compressor stability and efficiency. In the process

of designing slots, appropriate axial position should be considered firstly to improve the stall margin and reduce the efficiency loss. Although the axial position has been studied well, the study object was axial slots in most studies. Whether different effects will be shown by other type of slots, like blade angle slots? Besides, other studies only showed a rough variation of axial overlap. A detail and systematic variation of axial overlap is needed for an intensive study.

So, in this paper, the blade angle slots with six different axial overlap rates are investigated. In this investigation, two targets are expected. Firstly, the effects of different axial overlaps on the compressor stability and efficiency will be revealed. Secondly, the internal mechanism of blade angle slots with different axial overlaps will be clarified. By this study, the design guide line of slots will be further enriched.

## 2. RESEARCH OBJECT AND METHOD

### 2.1 Test Rig and Casing Treatments

In this paper, all the investigations are carried out on an axial subsonic compressor rotor. The compressor test rig is located at Northwestern Polytechnical University, P. R. China. Figure 1 shows the structure diagram of the test rig. The test compressor rotor has 30 blades, and the casing diameter is 298mm, with the tip clearance gap of 0.3mm. More design parameters of the test compressor rotor are shown in Table 1. In this investigation, the rotational speed of the test compressor rotor is 10765rpm. According to the past study ([Wu \*et al.\* 2012](#)), the compressor with smooth wall (SW) has a spike stall-inception, and the blockage of the tip channel caused by the tip leakage flow (TLF) is the main stall reason.

**Table 1 Design parameters of the rotor**

Parameter	Value
Design rotational speed (rpm)	15200
Design mass flow rate (kg/s)	5.6
Design total pressure ratio	1.249
Design isentropic efficiency	0.905
Number of blades	30
Casing diameter (mm)	298
Tip clearance/Tip chord	0.011
Hub-tip ratio	0.61

A skew blade angle slot is chosen as the casing treatment in this study. Different from the axial slots, the studied slots skew in axial and radial directions. Figure 2 shows the detail structure of the blade angle slots. A parameter, axial overlap rate, is used to represent the position of slots in the tip. The axial overlap rate is the ratio of the covering length to the tip axial chord length. By changing the axial overlap rate, six different slots are designed to investigate, with the axial overlap rate of 0.2, 0.3, 0.4, 0.6, 0.8 and 1.0 (denoted with AS\_0.2, AS\_0.3, AS\_0.4, AS\_0.6, AS\_0.8 and AS\_1.0). In the past study (Zhang *et al.* 2019), the slot with 0.4 axial overlap rate has been investigated, so this slot is as the baseline slot geometry to perform the computational parametric study. The detail geometrical parameters of slots are shown in table 2.

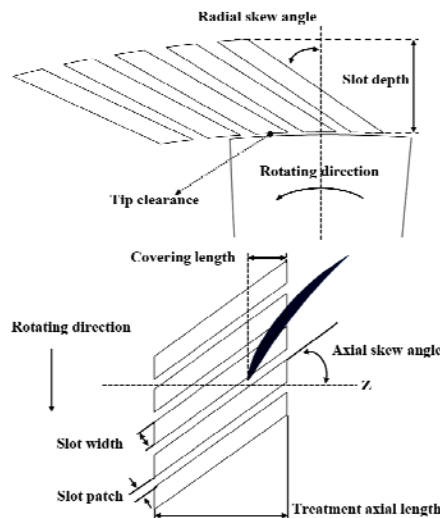


Fig. 2. Detail structure diagram of casing treatments.

Table 2 Geometrical parameters of slot casing treatments

Parameter	Value
Slot number of full annulus	150
Slot width/Slot patch	2.21
Slot depth/mm	13
Axial skew angle/degree	37.1
Radial skew angle/degree	60

## 2.2 Numerical Scheme

The commercial CFD software, NUMECA (2001), was utilized to perform the unsteady numerical simulation. The k-epsilon turbulence model was used in the process of solving the Reynolds time-averaged Navier-Stokes equations. In the steady calculations, an explicit four-stage Runge-Kutta scheme with local time step was utilized. In the unsteady calculations, the spatial discretization adopted upwind TVD scheme with second-order precision, and the implicit dual time stepping

method were utilized. According to the past study experience (Zhang *et al.* 2019), within one rotor blade pitch, the physical time steps were set to 20, and the virtual time steps in each physical time step were also set to 20. The convergent results were obtained after at least six complete rotation cycles, with the mass flow, total pressure and efficiency keep changing periodically. To reduce the cost of calculated time, local time step, implicit residual smoothing and multi-grid schemes were utilized. The inlet boundary conditions were given the direction of the inlet airflow, the total pressure is 101325 Pa, and the total temperature is 288.2 K. The average static pressure is given in the outlet boundary. By varying the outlet average static pressure, near-stall mass flow point and other mass flow points were obtained. No-heat transfer and no-slip conditions were assumed in the solid surface of the casing, hub and blades.

The structured grid and the grid partition technology were applied in the compressor channel. HOH grid topology was adopted in the rotor channel, and the grid nodes in the radial, tangential and axial directions were 69, 57 and 233 respectively. In the tip clearance, the butterfly grid topology was adopted, with 17 grid nodes in radial direction. For inlet/outlet extensions and blade angle slots, H grid topology was adopted, with 41 radial nodes, 21 tangential nodes and 57 axial nodes. And the total number of grids in the calculation of single channel were about 1.4 million. Figure 3 shows the grid distribution of the compressor meridian plane. The compressor channel is divided into two parts, stationary part and rotating part. The stationary part contains the inlet extension and slots, and the rotating part contains the rotor channel and outlet extension. It is worth noting that the turbulence model and the number of grids used in this paper have been verified in the previous researches (Zhang *et al.* 2010; Zhang *et al.* 2019). So, the turbulence model and grid independence verification are no longer carried out in this paper.

## 2.3 Verification for Numerical Scheme

Figure 4 shows the experimental and calculated overall performance of the rotor at part design speed of 10765 rpm. The corrected mass flow rate of different operation points is dimensionless by the maximum corrected mass flow rate of smooth wall in the experiment. It can be seen that the calculated results can be in good agreement with the experimental results. The calculated total pressure ratio is basically consistent with the experimental values. The error between calculated and experimental near-stall mass flow rates is within 2.5%. In addition, the calculated efficiency has some differences compared with the experimental value. At the large mass flow rate, the calculated efficiency is higher than the experimental value. At the medium and small mass flow rate, the calculated efficiency is slightly smaller than the experimental value. The maximum relative error of efficiency between calculation and experiment is around 4%.

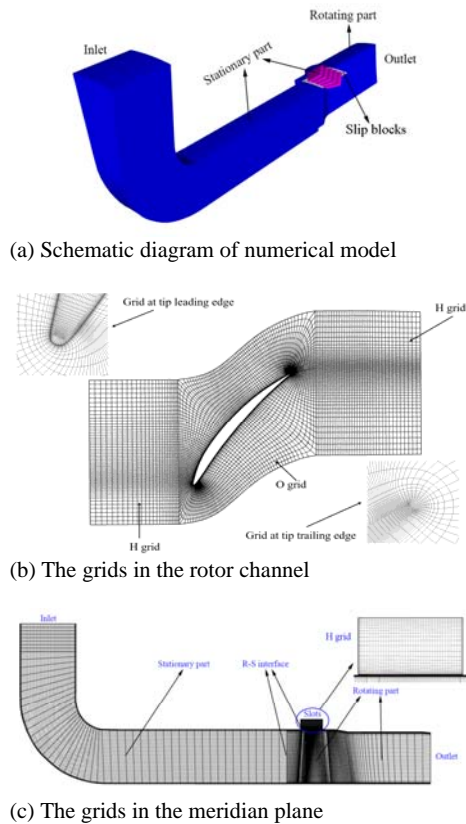


**Fig. 3. Schematic diagram and grids of numerical model.**

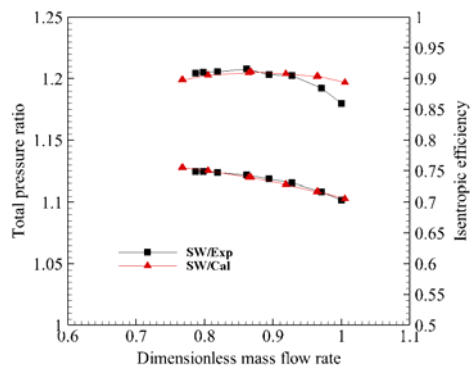


**Fig. 4. Overall performance of the rotor at part design speed.**

Figure 5 shows the distribution of the total pressure ratio and the outlet absolute flow angle along the blade span at the peak efficiency point. It can be seen that the calculated results can correctly predict the variation trends of the experimental results. The calculated flow parameters distribution along the span are in good agreement with the experimental results, especially the outlet absolute flow angle near the tip. There are some differences between the calculated overall performance and the experimental results. The reasons may be that the turbulence model is not accurate enough, and the numerical calculation of the compressor model is

different from the actual compressor or the measurement error. Although the differences exist, the current accuracy of the numerical simulation is enough to reveal the internal flow mechanism of the effects of different slots on the compressor stability.

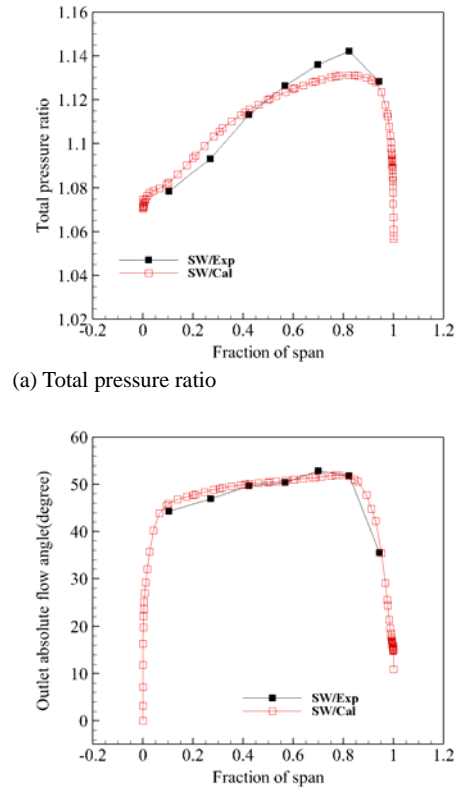


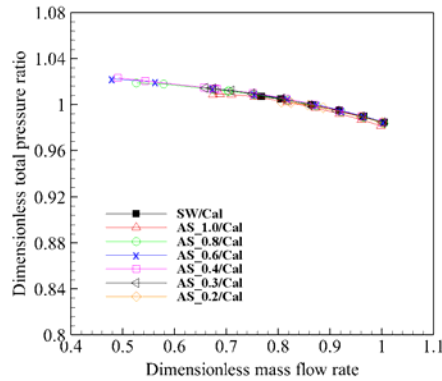
**Fig. 5. Distribution of total pressure ratio and outlet absolute flow angle at peak efficiency point.**

### 3. RESULTS AND DISCUSSIONS

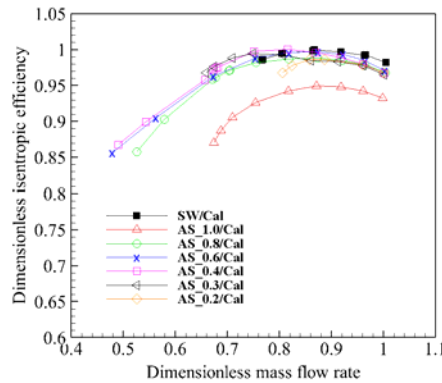
#### 3.1 Analysis of Compressor Performance

This study is aimed to reveal the effects of different axial overlap rates of the slot casing treatments on the stability and internal flow field of the compressor at part design speed. Thus, Figure 6 shows the overall performance of the compressor with different slot casing treatments. The mass flow rate of different operation points is dimensionless by the maximum mass flow rate of SW in the experiment, and the total pressure ratio and isentropic efficiency of different operation points are dimensionless by the total pressure ratio and isentropic efficiency of the peak efficiency point of SW in the calculation. It can be seen that the AS\_0.3, AS\_0.4, AS\_0.6, AS\_0.8 and AS\_1.0 decrease the stall mass flow of the compressor, and the AS\_0.6 obtains the largest decrease of the stall mass flow. However, the AS\_0.2 increases the stall mass flow of the compressor. For the compressor efficiency, slot casing treatments with different

axial overlap rates decrease the peak efficiency besides the AS\_0.4. Especially, the AS\_1.0 causes an obvious and large efficiency penalty.



(a) Dimensionless total pressure ratio



(b) Dimensionless isentropic efficiency

**Fig. 6. Overall performance of different slots at part design speed.**

This paper introduces the definition of stall margin improvement(SMI) and peak efficiency loss(PEL) to quantify the effect of casing treatment on compressor stability and efficiency. The detail definitions are as follows:

$$SMI = \left[ \left( \frac{\pi_{ct, stall}^*}{\pi_{sw, stall}^*} \right) \cdot \left( \frac{M_{sw, stall}}{M_{ct, stall}} \right) - 1 \right] \times 100\% \quad (1)$$

$$PEL = \left[ \left( \eta_{sw, peak}^* - \eta_{ct, peak}^* \right) / \eta_{sw, peak}^* \right] \times 100\% \quad (2)$$

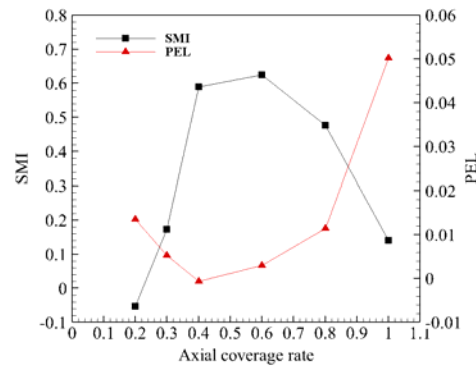
where  $\pi_{ct, stall}^*$  is the total pressure ratio of the near stall point with casing treatment,  $\pi_{sw, stall}^*$  is the total pressure ratio of the near stall point with smooth wall,  $M_{ct, stall}$  is the mass flow rate of near stall point with casing treatment,  $M_{sw, stall}$  is the mass flow rate of near stall point with smooth wall,  $\eta_{ct, peak}^*$  is the peak efficiency with casing treatment and  $\eta_{sw, peak}^*$  is the peak efficiency with smooth wall.

Table 3 lists the concrete data of SMI and PEL,

besides, the dimensionless mass flow rate(DMF) of near stall point for different shrouds is also given. The listed data indicate that the AS\_0.6 obtain the largest stall margin improvement of 62.51% with peak efficiency penalty of 0.30%. Consider of taking into account both stability and efficiency, the AS\_0.4 should be more excellent, which obtained 58.86% stall margin improvement with 0.07% peak efficiency improvement. When axial overlap rate at the range of 0.3 to 1.0, blade angle slots decrease the stall mass flow rate compare with smooth wall; however, when axial overlap rate is 0.2, the slots increase the stall mass flow rate and make negative effect on the compressor stability. Figure 7 shows the variation tendency of SMI and PEL along with axial overlap rate. It demonstrates that the slot casing treatment exist the optimal axial overlap rate to obtain the largest stall margin improvement and the lowest peak efficiency loss. When axial overlap rate is too less or large, it has adverse effect on compressor stability and efficiency.

**Table 3 Stall margin improvement and peak efficiency loss for calculation**

Case	DMF at near-stall point	SMI/%	PEL/%
SW	0.767	/	/
AS_1.0	0.674	14.01	5.02
AS_0.8	0.526	47.63	1.14
AS_0.6	0.479	62.51	0.30
AS_0.4	0.491	58.86	-0.07
AS_0.3	0.659	17.30	0.53
AS_0.2	0.806	-5.28	1.35



**Fig. 7. Variation tendency of SMI and PEL.**

In order to further clarify the internal flow mechanism of slot casing treatments with different axial overlap rates, the detail analysis of flow field in the compressor will be carried out.

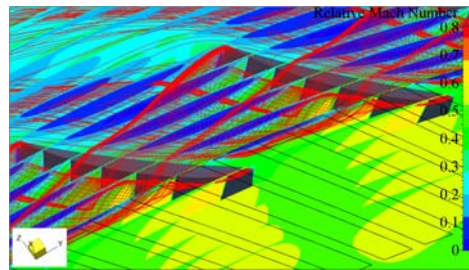
### 3.2 Analysis of flow Field in the Compressor

#### 3.2.1 The Effect of Different Axial Overlap Rates on Compressor Stability

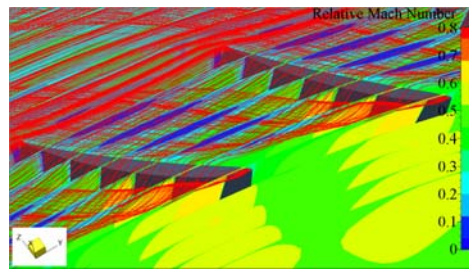
##### *Negative effect on the compressor stability*

In the analysis of compressor performance, the

results demonstrate that the AS\_0.2 made negative effect on the compressor stability. Figure 8 shows the distributions of relative Mach number and the streamline of clearance leakage flow near the tip channel at 0.806DMF for AS\_0.2 and SW. It is apparent that the low velocity region, which is blue near the tip channel, increased after the AS\_0.2 is applied, meanwhile the tip leakage vortex expands and fills with the entire tip channel. In Fig. 9, the positive dimensionless radial velocity ( $V_r$ ) represent the bleeding flows in the open surface of slots. The dimensionless  $V_r$  is defined as the ratio of the local radial velocity to the averaged outlet axial velocity. Figure 9 reveals that the bleeding flows formed in the slot is weak, as most dimensionless  $V_r$  values are less than 0.1, and the position of bleeding flows covers less of the front part of TLF. Besides, the interference of slots makes the tip leakage flow more turbulent.



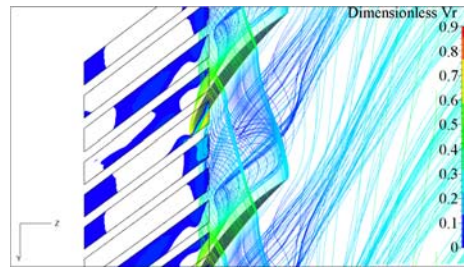
(a) AS\_0.2



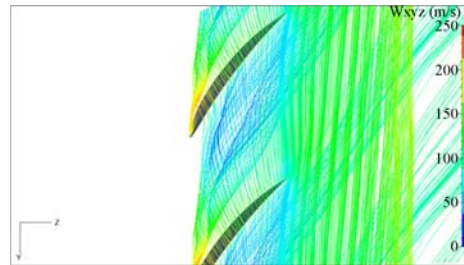
(b) SW

**Fig. 8. Distributions of relative Mach number and tip leakage flow streamline.**

The detail flow field of three instants in the slots are shown in Fig. 10, such as the streamline in one slot section, the distribution of dimensionless static pressure in the bottom of one slot and the local relative Mach number in slot and tip channel. The dimensionless static pressure is defined as the ratio of local static pressure to 101325Pa. It can be seen that the relative Mach numbers in the slots are very small, which indicates that the bleeding-injection effect in the slot is weak. The difference of dimensionless static pressure in the bottom of slots is the driving force of forming the bleeding-injection flow in the slots. At three instants of 0.3T, 0.6T and 0.9T, due to the position of bleeding flows covers less of the front part of TLF, the bleeding flows has no actual removing effect on the tip leakage flow.

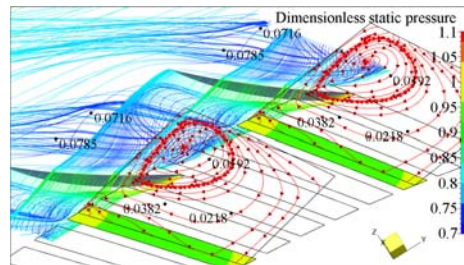


(a) AS\_0.2

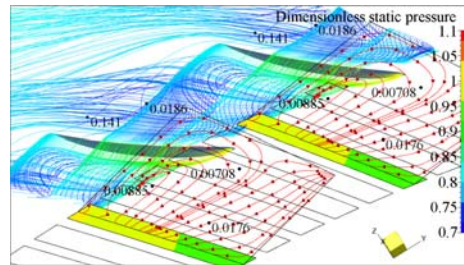


(b) SW

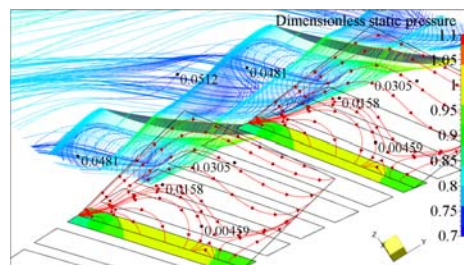
**Fig. 9. Distribution of bleeding flows in the open surface of slots.**



(a) 0.3T



(b) 0.6T

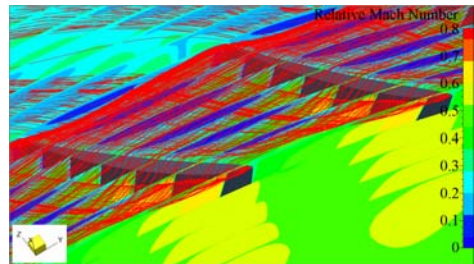


(c) 0.9T

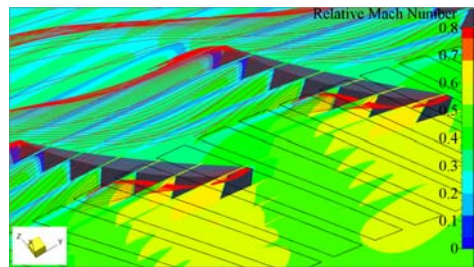
**Fig. 10. Flow field in the slots of AS\_0.2.**

By the analyses above, there are two main reasons that the AS\_0.2 makes negative effect on

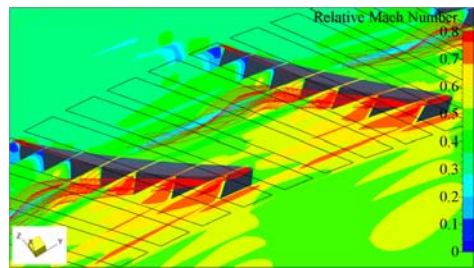
compressor stability. One reason is that the bleeding flows forming in the slots is weak, another reason is that the position of bleeding flows covers less of the front part of TLF. That why the slots with 0.2 axial overlap rate cannot actually remove the tip leakage flow. On the other hand, the results reveal the critical role of axial position of slots on extending stability.



(a) SW



(b) AS\_0.4



(c) AS\_1.0

**Fig. 11. Distributions of relative Mach number and tip leakage flow streamline.**

**Positive effect on the compressor stability**

According to the above analysis of compressor performance, the AS\_0.3, AS\_0.4, AS\_0.6, AS\_0.8 and AS\_1.0 can improve the stall margin of compressor. To reveal the flow mechanism of stall margin improvement, two typical slots of AS\_0.4 and AS\_1.0 are chosen to compare with SW. Figure 11 shows the distributions of relative Mach number and the streamline of clearance leakage flow near the tip channel at 0.767 DMF, which the SW is near the stall condition. It can be seen clearly that the tip channel is filled with the adverse clearance leakage flow for SW, and large scale blue low speed region appears in the tip channel. When the slots are applied, quantity of the tip leakage flow and low speed region is obviously decreased. However, the remained tip leakage flow for AS\_1.0 is more than

that for AS\_0.4. It reveals that the slots with 0.4 axial overlap rate have more effective capacity in removing tip leakage flow than the slots with 1.0 axial overlap rate. In other words, different axial overlap rates can make slots behave different capacity on removing tip leakage flow.

The blockage of tip channel caused by tip leakage flow is the key reason of stall inception. Figure 11 indicates that the slots can decrease the blockage by removing tip leakage flow. And it is also proved by Fig. 12, which shows the extent of flow blockage of 99% span for SW and five different slots at 0.767 DMF. The extent of flow blockage is defined by the percent of flow blockage area (where  $V_z < 0$ ) accounting for total flow channel area. It can be seen that the flow blockage of tip channel is decreased after applying the slots with over 0.3 axial overlap rate. And the extent of flow blockage in the tip channel can reach the minimum value with appropriate axial overlap rate. Besides, the magnitude of bleeding and injection flow in the slots at 0.767 DMF is shown in the Fig. 13. The mass flow of bleeding and injection flow is dimensionless by inlet mass flow of compressor. It shows that with the increase of axial overlap rate, the magnitude of bleeding and injection flow also increases. It also means that the intensity of bleeding and injection effect increases with the increase of axial overlap rate. The larger intensity of bleeding and injection effect generates larger potential capacity of removing tip leakage flow. However, the larger potential capacity of removing tip leakage flow does not mean that larger stall margin improvement can be obtained, which can be inferred by the above analysis of compressor performance. The relative position of slots and tip leakage flow is another influence factor to the stall margin improvement of compressor.

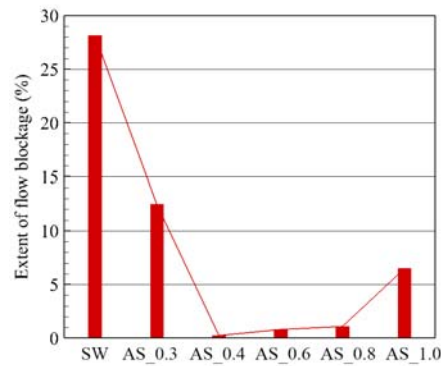


**Fig. 12. Extent of flow blockage at 99% span.**

In order to reveal the inherent relation between axial overlap rate and stall margin improvement, Figure 14 shows the distribution of bleeding flows in the open surface of slots and the tip leakage flow in the channel at 0.767 DMF. The positive values of dimensionless  $V_r$  represent the bleeding flows forming in the slots. It can be seen that the bleeding position covered the front part of TLF for the slots with 0.4 axial overlap rate. Differently, for the slots

with 1.0 axial overlap rate, the bleeding position covered the rear part of TLF. The value of dimensionless  $V_r$  and area of bleeding flows for AS\_1.0 are larger than that for AS\_0.4. Besides, the axial scale of tip leakage vortex for AS\_1.0 is also larger than that for AS\_0.4.

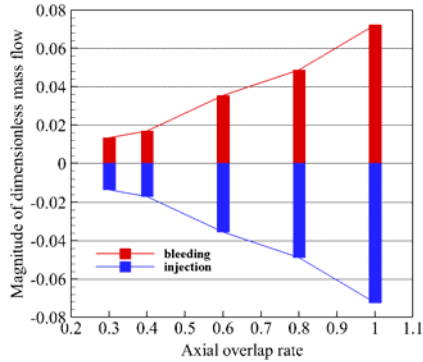
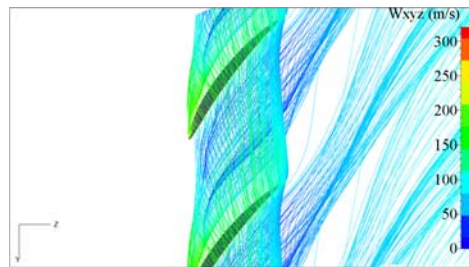
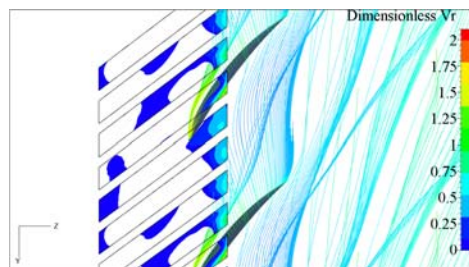


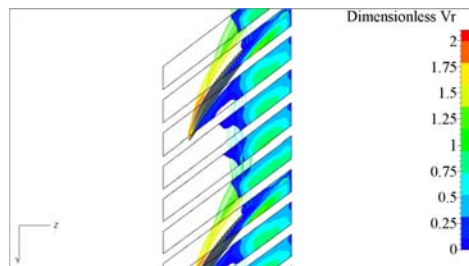
**Fig. 13. Magnitude of bleeding and injection flow in the slots.**



(a) SW



(b) AS\_0.4

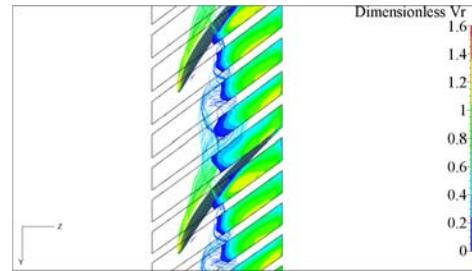


(c) AS\_1.0

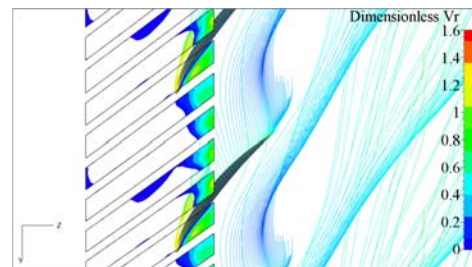
**Fig. 14. Distribution of bleeding flows in the open surface of slots.**

For further analysis, the distribution of bleeding flows and tip leakage flow in the open surface of slots at 0.674DMF are given in Fig. 15. When the

compressor with AS\_1.0 is near stall condition, the initial location of bleeding flows is almost behind tip leakage vortex and tip leakage vortex breakdown before the initial location of bleeding flows. Although the strong intensity of bleeding flows forms in the slots, the little tip leakage flow can be removed. As a result, the tip channel is blocked up with the adverse leakage flow. However, in the Fig.15(b), the bleeding flows in the slots can covers the front part of TLF, and the adverse tip leakage flow can be removed effectively by AS\_0.4. So, AS\_0.4 generates larger stall margin improvement than AS\_1.0.



(a) AS\_1.0



(b) AS\_0.4

**Fig. 15. Distribution of bleeding flows in the open surface of slots.**

According to above analyses, with the change of axial overlap rate, the relative position of bleeding flows in the slots and the front part of TLF is the critical influence factor to the stall margin improvement of compressor. If the bleeding flows in the slots can cover the front part of TLF, great stall margin improvement usually can be generated. To explain this influence, Fig. 16 shows the axial distribution of the circumferential averaged radial velocity in the open surface of slots at 0.767DMF. The positive radial velocity can represent the bleeding flows, and the location and range of zero points also represent the location and range of bleeding flows. Besides, the tip leakage velocity also shows in Fig.16, which is dimensionless by inlet averaged axial velocity. The dimensionless tip leakage velocity can represent the intensity of tip leakage flow, and the larger dimensionless tip leakage velocity means the tip leakage flow with higher energy. The two vertical curves represent the leading edge and trailing edge of tip. It can be seen from Fig. 16 that the front part of TLF near the leading edge has high energy, and the larger axial overlap rate is, the latter bleeding position of slots is. Moreover, the bleeding flows of AS\_0.4 and AS\_0.6 can cover most front part of TLE with high

energy, and great stall margin improvements are obtained. The bleeding flows of AS\_0.8 and AS\_1.0 only cover the most rear part of TLF with low energy, so the stall margin improvement is decreased. For AS\_0.3, the range and intensity of bleeding flows covered high energy TLF are less than these of AS\_0.4. It is the probable reason that the SMI of AS\_0.3 is less than the SMI of AS\_0.4.

To reveal the effect of slots on the tip leakage velocity, Fig. 17 shows the axial distribution of dimensionless tip leakage velocity at 0.767DMF. The two vertical curves represent the leading edge and trailing edge of tip. When the compressor with SW is near stall, the front part of TLF has high energy. After the AS\_0.4 is applied, the intensity of TLF near leading edge decreases obviously, and the rear part of TLF also decreases. However, when the AS\_1.0 is applied, the intensity of TLF near leading edge is still strong, but the rear part of TLF decreases. This difference is due to the difference of relative position of bleeding flows in the slots and the front part of TLF. The bleeding flows in the slots covers more the front part of TLF with high energy, more stall margin improvement can be generated. So, AS\_0.4 can obtain larger SMI than AS\_1.0.

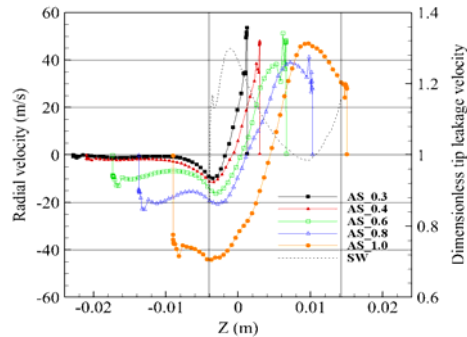


**Fig. 16. Circumferential averaged radial velocity in the open surface of slots and the dimensionless tip leakage velocity.**

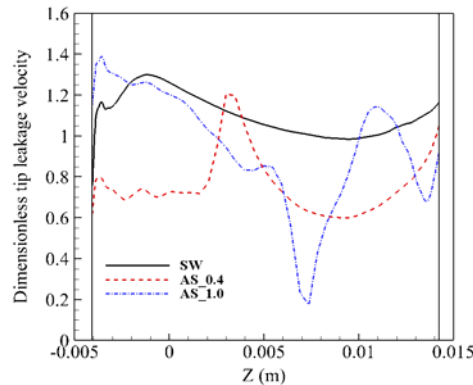
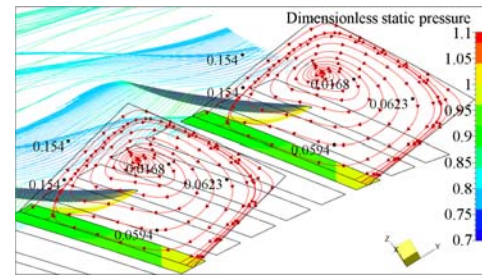


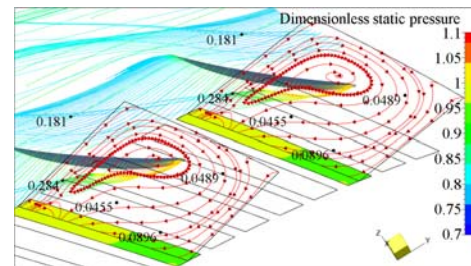
**Fig. 17. Axial distribution of dimensionless tip leakage velocity.**

The detail flow field of three instants in the slots of AS\_0.4 and AS\_1.0 are shown in Fig. 18 and 19. According to these two figures, it can be observed

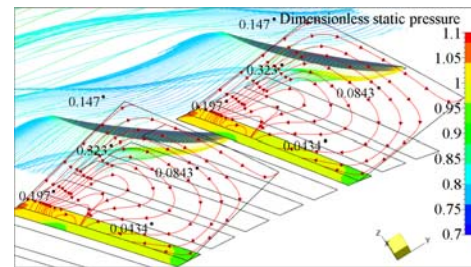
that the bleeding and injecting recirculated flows formed in the slots. The recirculated flows in the slots plays an important role in removing the adverse tip leakage flow. When the slots with 0.4 axial overlap rate, as shown in the Fig. 18, the position of bleeding flows in the slots is near the front part of TLF. Under the effect of bleeding flows, the leakage flow decreases obviously in the tip channel. When the slots with 1.0 axial overlap rate, as shown in the Fig. 19, the position of bleeding flows in the slots is near the rear part of tip leakage flow. Under the effect of bleeding flows, less leakage flow can be removed by slots. And the remained tip leakage flow is far away the position of bleeding flows. Besides, by comparing the local values of relative Mach number in the slots, the intensity of bleeding-injection effect for AS\_0.4 is weaker than that for AS\_1.0, which is consistent with Fig. 13. However, the SMI for AS\_0.4 is more than that for AS\_1.0. The results also indicate that the relative position of bleeding flows in the slots and tip leakage flow plays a critical role in extending instability boundary.



(a) 0.3T



(b) 0.6T

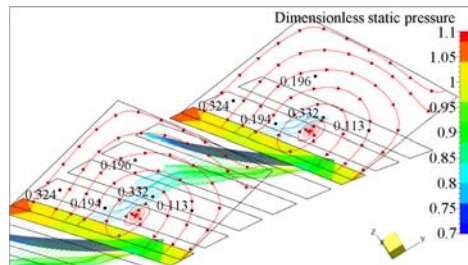


(c) 0.9T

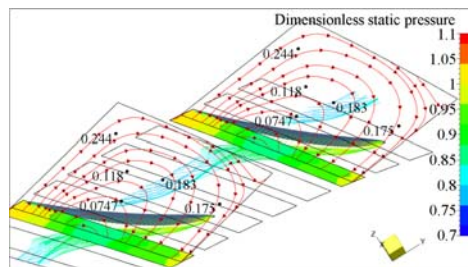
**Fig. 18. Distribution the flow field in the slots of AS\_0.4.**

In summary, the blockage of tip channel caused by adverse tip leakage flow is the critical reason of compressor stall inception. In the variation of the axial overlap rate, the relative position of bleeding

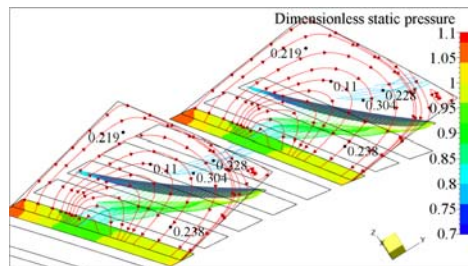
flows in the slots and tip leakage flow is the most important factor for stall margin improvement. To removing the tip leakage flow effectively, the front part of TLF with high energy should be covered by bleeding flows. The intensity of recirculated flows is second important factor for stall margin improvement.



(a) 0.3T



(b) 0.6T



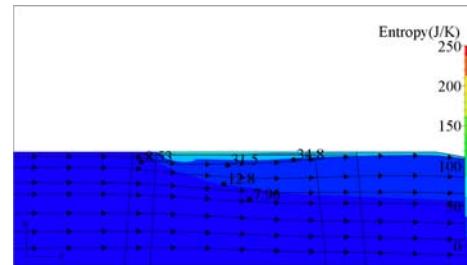
(c) 0.9T

**Fig. 19. Distribution the flow field in the slots of AS\_1.0.**

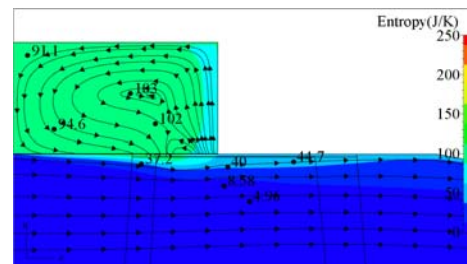
### 3.2.2 The Effect of Different Axial Overlap Rates on Compressor Efficiency

When the slots casing treatment is applied in the compressor, the interaction between the recirculated flows in the slots and the main flows of the compressor passage causes a certain loss inevitably. To reveal the effect of different slots on compressor efficiency, the entropy distribution and streamlines in the meridian plane at 0.767DMF are given in the Fig. 20. After the slots are applied, the high entropy region appears near the tip channel. The range of high entropy region of AS\_1.0 is larger than that of AS\_0.4. And the maximum entropy value of AS\_0.4 is more than that of AS\_1.0. Due to the recirculation in the slots, the vortex forms in the slots. For AS\_0.4, the vortex core is inside the slots and far from tip channel. However, for AS\_1.0, the vortex core is near the tip channel and the high entropy values in the vortex core bring much flow

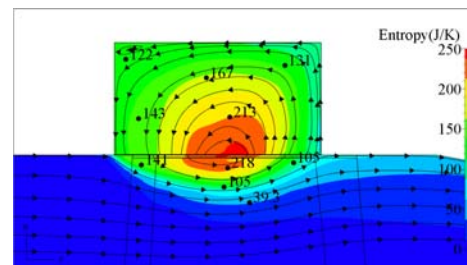
losses. Meanwhile, the integral of circumferential averaged entropy in the meridian plane is calculated to quantify the flow losses. As shown in Fig. 21, the slots with appropriate axial overlap rate can decrease flow losses of compressor, such as AS\_0.3 and AS\_0.4. With the further increase of axial overlap rate, the flow losses in the compressor increases, and the flow losses is larger than that for SW. So, the efficiency of compressor decreases due to the increase of flow losses.



(a) SW



(b) AS\_0.4



(c) AS\_1.0

**Fig. 20. Distribution of entropy and streamlines in the meridian plane.**

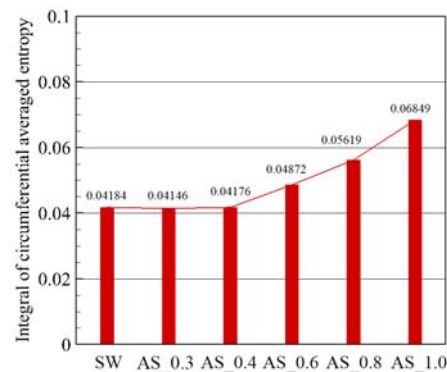
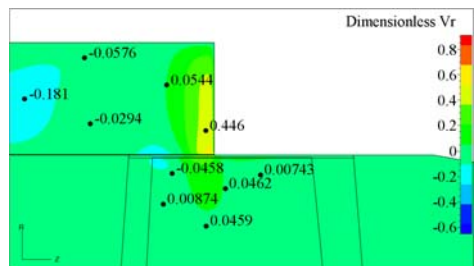


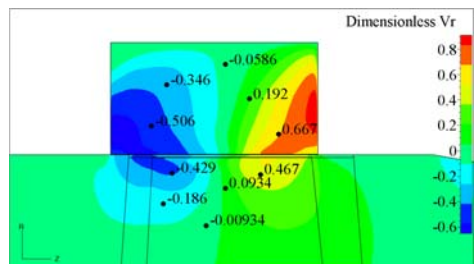
**Fig. 21. Integral of circumferential averaged entropy with different slots.**

To further reveal the effect on efficiency, the distribution of dimensionless  $V_r$  in the meridian plane at 0.767DMF is given in Fig. 22. It is apparent that the absolute values of the dimensionless  $V_r$  for AS\_0.4 in the slots and tip channel are lower than those for the AS\_1.0. On the one hand, the intensity of recirculated flows in the slots increases with the increase of axial overlap rate; on the other hand, the range of the slots covering tip channel increases with the increase of axial overlap rate. Hence, the intensity and range of interaction between recirculated flows and main flows increases with the increase of axial overlap rate. As a result, more flow losses are caused.

In summary, when axial overlap rate is over 0.4, the slots with larger axial overlap rate will cause larger intensity and range of interaction between recirculated flows and main flows, so more flow losses are caused. In the design of slots casing treatment, appropriate axial overlap rate should be considered to obtain enough stall margin improvement with least efficiency loss.



(a) AS\_0.4



(b) AS\_1.0

**Fig. 22. Distribution of dimensionless radial velocity in the meridian plane.**

#### 4. CONCLUSION

In this paper, six kinds of blade angle slot casing treatments with different axial overlap rates are investigated on a subsonic axial flow compressor rotor by unsteady numerical simulations. The effects on the compressor stability and internal mechanism of blade angle slots with different axial overlaps are clarified. Several conclusions are summarized as follows:

1. The tip blockage caused by the adverse tip leakage flow is the critical factor of the inception of compressor stall. By applying blade angle slots casing treatment, the stall margin of compressor can be improved. The internal mechanism is that

the recirculated flows formed in the slots can bleed and remove the tip leakage flow, and the tip channel blockage is reduced by restraining the tip leakage flow.

2. The blade angle slots with different axial overlap rates behave different effects on the compressor stability. With the increase of the axial overlap rate of blade angle slots, the improvement of compressor stability firstly increased and then decreased. The relative position between bleeding flows in the slots and tip leakage flow is the most important factor for the stall margin improvement. When the front part of the TLF with high energy can be covered by bleeding flows, the adverse tip leakage flow can be removed more effectively, and greater stall margin improvement can be obtained. When the axial overlap is smaller or larger than that of optimal blade angle slot, the ability of bleeding flows to remove high energy TLF is weakened. So, the stall margin improvement is also decreased.
3. The interaction between the recirculated flows in the slots and the main flows of the compressor passage causes flow losses inevitably. With the increase of the axial overlap rate from 0.4, the intensity and range of interaction between recirculated flows and main flows will become larger, and more flow losses will be generated. However, the blade angle slots with appropriate axial overlap rate can cause least flow losses.

#### ACKNOWLEDGEMENTS

The authors thank for the supports by National Science Foundation of China with project No.51006084. This research also is supported by National Science and Technology Major Project No.2017-II-0005-0018 and the Fundamental Research Funds for the Central Universities with project No.3102019ZX026.

#### REFERENCES

- Benser, W. A. and H. B. Finger (1957). Compressor Stall Problems in Gas-Turbine-Type Aircraft Engines. *SAE Transactions*, 187-200.
- Brandstetter, C., F. Wartzek, J. Werner, H. P. Schiffer and F. Heinichen (2016). Unsteady measurements of periodic effects in a transonic compressor with casing treatments. *Journal of Turbomachinery* 138(5).
- Brignole, G. A., F. C. Danner and H. P. Kau (2008, January). Time resolved simulation and experimental validation of the flow in axial slot casing treatments for transonic axial compressors. In *ASME Turbo Expo 2008: Power for Land, Sea, and Air* (pp. 363-374). American Society of Mechanical Engineers Digital Collection.
- Danner, F. C., H. P. Kau, H. P. Schiffer and G. A. Brignole (2009, January). Experimental and

- numerical analysis of axial skewed slot casing treatments for a transonic compressor stage. In *ASME Turbo Expo 2009: Power for Land, Sea, and Air* (pp. 227-238). American Society of Mechanical Engineers Digital Collection.
- Djehghri, N., H. D. Vo and H. Yu (2015, June). Parametric study for lossless casing treatment on a mixed-flow compressor rotor. In *ASME Turbo Expo 2015: Turbine Technical Conference and Exposition*. American Society of Mechanical Engineers Digital Collection.
- Fujita, H. and H. Takata (1984). A study on configurations of casing treatment for axial flow compressors. *Bulletin of JSME* 27(230), 1675-1681.
- Greitzer, E. M. (1976a). Surge and rotating stall in axial flow compressors—Part I: Theoretical compression system model. *Journal of Engineering for Power* 98(2), 190-198.
- Greitzer, E. M. (1976b). Surge and rotating stall in axial flow compressors—Part II: experimental results and comparison with theory. *Journal of Engineering for Power* 98(2), 199-211.
- Guruprasad, S. A. (1999). Experimental investigations on the influence of axial extension and location of outer casing treatment on the performance of an axial flow compressor. In *Fourth international symposium on experimental and computational aerothermodynamics of internal flows* (Dresden, August 31-September 2 1999).
- Hembera, M., F. Danner, H. P. Kau and G. Brignole (2008). Numerical design and optimization of casing treatments for transonic axial compressors. In *44th AIAA/ASME/SAE/ASEE Joint Propulsion Conference & Exhibit* (p. 5063).
- Koch, C. C. (1970). Experimental evaluation of outer case blowing or bleeding of single stage axial flow compressor, part 6 Final report.
- Kuang, H., W. Chu, H. Zhang and S. Ma (2017). Flow mechanism for stall margin improvement via axial slot casing treatment on a transonic axial compressor. *Journal of Applied Fluid Mechanics* 10(2).
- Lin, F., F. Ning and H. Liu (2008, January). Aerodynamics of Compressor Casing Treatment: Part I—Experiment and Time-Accurate Numerical Simulation. In *ASME Turbo Expo 2008: Power for Land, Sea, and Air* (pp. 731-744). American Society of Mechanical Engineers Digital Collection.
- Liu, Z., C. Zhang, J. Shi, Z. Wang and J. Huang (1987). A study on effects of axial positions of skewed slots casing treatment on compressor performance. *Journal of Engineering and Thermophysics* 8, 52-54.
- Lu, J., W. Chu and Y. Wu (2009, January). Investigation of skewed slot casing on transonic axial-flow fan stage. In *ASME Turbo Expo 2009: Power for Land, Sea, and Air* (pp. 133-144). American Society of Mechanical Engineers Digital Collection.
- Lu, X., W. Chu, Y. Zhang and J. Zhu (2006). Experimental and numerical investigation of a subsonic compressor with bend-skewed slot-casing treatment. *Proceedings of the Institution of Mechanical Engineers, Part C: Journal of Mechanical Engineering Science* 220(12), 1785-1796.
- Muller, M. W., H. P. Schiffer, M. Voges and C. Hah (2011, January). Investigation of passage flow features in a transonic compressor rotor with casing treatments. In *ASME 2011 turbo expo: Turbine technical conference and exposition* (pp. 65-75). American Society of Mechanical Engineers.
- NUMECA Inc (2011). *NUMECA Theoretical Manual-FINE Turbo*. Brussels, BE.
- Prince, D. C., D. C. Wisler and D. E. Hilvers (1975, March). A study of casing treatment stall margin improvement phenomena. In *ASME 1975 International Gas Turbine Conference and Products Show* (pp. V01AT01A059-V01AT01A059). American Society of Mechanical Engineers.
- Wilke, I. and H. P. Kau (2003, January). A numerical investigation of the flow mechanisms in a HPC front stage with axial slots. In *ASME Turbo Expo 2003, collocated with the 2003 International Joint Power Generation Conference* (pp. 465-477). American Society of Mechanical Engineers Digital Collection.
- Wilke, I., H. P. Kau and G. Bri Gnole (2005, January). Numerically aided design of a high-efficient casing treatment for a transonic compressor. In *ASME turbo expo 2005: Power for land, sea, and air* (pp. 353-364). American Society of Mechanical Engineers Digital Collection.
- Wu, Y., Q. Li, J. Tian and W. Chu (2012). Investigation of pre-stall behavior in an axial compressor rotor—Part I: Unsteadiness of tip clearance flow. *Journal of Turbomachinery* 134(5), 051027.
- Zhang, H., W. Chu and Y. Wu (2011). Mechanism of influences of axial positions of axial skewed slot casing treatment on a compressor performance. *Journal of Aerospace Power* 1.
- Zhang, H., W. Chu, Y. Wu and Z. Su (2010). Investigation of the flow mechanisms of affecting compressor performance with axial skewed slots casing treatment. *Journal of Propulsion Technology* 31(5), 555-561.
- Zhang, H., W. Liu, E. Wang, Y. Wu and W. Yao (2019). Mechanism investigation of enhancing the stability of an axial flow rotor by blade angle slots. *Proceedings of the Institution of Mechanical Engineers, Part G: Journal of*

*Aerospace Engineering.*

Zhou, X., Q. Zhao, W. Cui and J. Xu (2017). Investigation on axial effect of slot casing treatment in a transonic compressor. *Applied Thermal Engineering* 126, 53-69.

Zhu, J. and W. Chu (2005, January). The effects of bend skewed groove casing treatment on performance and flow field near endwall of an axial compressor. *In 43rd AIAA Aerospace Sciences meeting and exhibit* (p. 809).